Available online at www.sciencedirect.com
SCIENCE DIRECT®
International Journal of Pharmaceutics 292 (2005) 17–28
international journal of pharmaceutics
www.elsevier.com/locate/ijpharm

Hydrodynamics-induced variability in the USP apparatus II dissolution test

Jennifer L. Baxter, Joseph Kukura, Fernando J. Muzzio*

Department of Chemical and Biochemical Engineering, Rutgers University, 98 Brett Road, Piscataway, NJ 08854-8058, USA

Received 5 April 2004; received in revised form 6 August 2004; accepted 6 August 2004

Abstract

The USP tablet dissolution test is an analytical tool used for the verification of drug release processes and formulation selection within the pharmaceutical industry. Given the strong impact of this test, it is surprising that operating conditions and testing devices have been selected empirically. In fact, the flow phenomena in the USP test have received little attention in the past. An examination of the hydrodynamics in the USP apparatus II shows that the device is highly vulnerable to mixing problems that can affect testing performance and consistency. Experimental and computational techniques reveal that the flow field within the device is not uniform, and dissolution results can vary dramatically with the position of the tablet within the vessel. Specifically, computations predict sharp variations in the shear along the bottom of the vessel where the tablet is most likely to settle. Experiments in which the tablet location was carefully controlled reveal that the variation of shear within the testing device can affect the measured dissolution rate.

Keywords: Dissolution testing; Hydrodynamics; USP apparatus II; Shear; Computational fluid dynamics

1. Introduction

Drug dissolution testing is a critical component of pharmaceutical development and manufacturing. The design of new formulations is often guided and assessed based on in vitro dissolution rates. Moreover, the robustness and uniformity of manufacturing batches are determined using these same dissolution tests. Consequently, the reproducibility and accuracy of the dissolution tests, and identification of variability sources are of the utmost importance. Unfortunately, despite the reliance of the USP, the FDA, and the industry on dissolution testing, the hydrodynamics of the test are poorly understood and often produce inconsistent measurements. Failed dissolution tests resulted in 47 product recalls in 2000–2002, representing 16% of non-manufacturing recalls for oral solid dosage forms (FDC Reports, 2001, 2002, 2003). The financial consequences of a failed dissolution test can be substantial

* Corresponding author. Tel.: +1 732 445 3357.
E-mail address: muzzio@sol.rutgers.edu (F.J. Muzzio).

0378-5173/$ – see front matter © 2004 Published by Elsevier B.V.
doi:10.1016/j.ijpharm.2004.08.003

for a pharmaceutical corporation, necessitating product recalls, costly investigations and potential production delays.

Compounding the problem further, there have been numerous reports in the literature describing high variability of test results, even for dissolution apparatus calibrator tablets (Cox and Furman, 1982; Moore et al., 1995; Qureshi and Shabnam, 2001). The main hypothesis of this article is that much of this variability is caused by hydrodynamics. In the most common scenario, the USP apparatus II dissolution test is conducted in a small, agitated vessel operated at Reynolds numbers (*Re*) in the transitional regime.[1] Under such conditions, flow behavior in stirred tanks is known to be both time-dependent and strongly heterogeneous. As a result, the hydrodynamics in the vicinity of a tablet in the dissolution device would likely be both position and time-dependent. Fluctuations in the flow introduce variability in the evolution of processes that are affected by hydrodynamics, such as shearing of the tablet surfaces, de-agglomeration of particles, mass transfer from the solid to the liquid, suspension and mixing of tablet fragments.

Reports in the literature provide preliminary support for the hypothesis that hydrodynamics strongly influence in vitro dissolution testing. In 1962, Hamlin et al. (Hamlin et al., 1962) reported that the agitation rate has a strong effect on distinguishing differences in the measured dissolution rates of methylprednisolone forms I and II. Similarly, Levy et al. (Levy et al., 1965) showed that the sensitivity of the dissolution rate of a tablet to small changes in agitation intensity can yield in vitro results contrary to those obtained in vivo. Underwood and Cadwallder (Underwood and Cadwallder, 1976) showed that changes to the geometry, such as the size and shape of dissolution vessels and agitator position, can have a dramatic effect on the measured dissolution rate. Healy et al. (Healy et al., 2002) suggested that minor changes of the tablets (as measured by tablets of varying thicknesses) can result in significant differences in the rate of drug dissolution. Most of these studies focused on identifying factors that influence the ability to correlate in vitro and in vivo results rather than performing a focused analysis of the effect of the fluid motion. Only a few studies have been reported in the literature in which the focus was on evaluating and understanding the hydrodynamics of the fluid flow within the dissolution device. Mauger et al. (Mauger et al., 2003) used visualization studies with dye released from a non-disintegrating tablet coupled with intrinsic dissolution rate testing to characterize the flow in the USP apparatus II. Kamba et al. (Kamba et al., 2003) showed that the dissolution rate of constant release benzoic acid tablets increased with increasing agitation speed and distance from the center of the vessel bottom. Bocanegra et al. (Bocanegra et al., 1990) used laser doppler anemometry to collect velocity measurements at selected fixed locations within the apparatus II, however, the complete flow field and its mixing properties were not studied in detail. The flow field and mixing characteristics of the USP apparatus II are not well understood despite the aforementioned studies. The USP is currently evaluating potential changes to this test, and a comprehensive understanding of the hydrodynamics can provide significant contributions to aid in the evolution of this important tool.

In recent articles, Kukura et al. (Kukura et al., 2002, 2003) presented data which showed that under typical operating conditions, the USP apparatus II operates in a regime where the flow is highly time-dependent. These findings served as the foundation for the development of a preliminary computational model used to simulate the hydrodynamics within the USP II device. Using the preliminary model, the shear environment in the USP apparatus II was shown to be highly heterogeneous.

In this study, we develop and validate a rigorous computational model, and use it to understand hydrodynamic effects on dissolution in the USP apparatus II. The model allows for the calculation and evaluation of shear forces within the vessel, a quantity that cannot be easily measured experimentally. Shear represents an important factor for dissolution since the shear forces control the thickness of the boundary layer that limits mass transfer rates on tablet and particle surfaces. Positions along the vessel bottom are identified where the shear rate is minimum and maximum. Targeted experiments are conducted affixing three different tablet types at such positions to demonstrate the impact that non-uniform shear forces can have on dissolution measurements. Finally, a detailed statistical analysis is performed to demonstrate the statistical significance of tablet position on dissolution rate measurements.

[1] Reynolds number is traditionally defined as $Re = \rho ND^2/\mu$; where ρ is the fluid density, N the rotations per second of the agitator, D the agitator diameter, and μ is the fluid viscosity.

2. Materials and methods

2.1. Computational fluid dynamics

Commercially available computational fluid dynamics (CFD) tools can be used to model complex, three-dimensional mixing systems. After specification of the geometry of interest, the flow volume must be discretized into a mesh of finite elements (unstructured, tetrahedral elements are used in this work). A node is then placed at each corner of the tetrahedron and the generalized momentum balance, shown in Eq. (1), is solved at each nodal location in the discretized domain:

$$\frac{\partial(\rho u_i)}{\partial t} + \frac{\partial}{\partial x_j}(\rho u_i u_j) = -\frac{\partial p}{\partial x_i} + \frac{\partial}{\partial x_j}\left[\mu\left(\frac{\partial u_i}{\partial x_j} + \frac{\partial u_j}{\partial x_i} - \frac{2}{3}\frac{\partial u_k}{\partial x_k}\delta_{ij}\right)\right] + \rho g_i \quad (1)$$

In the turbulent regime, fluctuations in the mean velocity arise and these effects must be incorporated into the CFD model to ensure meaningful results (Kresta and Brodkey, 2004). This is accomplished through the use of a turbulence model. Most of these models rely on time averaging the conservation equations. After averaging, terms containing factors of the fluctuating component average to zero and the only remaining terms are those from the standard Navier–Stokes equations plus additional terms referred to as the Reynolds stresses. The resulting equation, shown in Eq. (2), is referred to as the Reynolds-averaged Navier–Stokes (RANS) equation:

$$\frac{\partial(\rho u_i)}{\partial t} + \frac{\partial}{\partial x_j}(\rho u_i u_j) = -\frac{\partial p}{\partial x_i} + \frac{\partial}{\partial x_j}\left[\mu\left(\frac{\partial u_i}{\partial x_j} + \frac{\partial u_j}{\partial x_i} - \frac{2}{3}\frac{\partial u_k}{\partial x_k}\delta_{ij}\right)\right] + \frac{\partial}{\partial x_j}(-\overline{\rho u_i' u_j'}) + \rho g_i \quad (2)$$

The Reynolds stresses need to be related to the other variables in the RANS to solve the system of equations. This is done through various models, typically referred to as turbulence models. For this body of work, the one-equation Sparlart–Allmaras closure model is used. Several comparative studies have been conducted in the literature evaluating this closure model relative to others and it was found to be among the best for overall performance (Bardina et al., 1997).

CFD modeling of the dissolution apparatus is performed using several software programs of known accuracy and reliability. The three-dimensional geometry specification and mesh generation are accomplished using ICEM-CFD (ICEM CFD Engineering, Berkeley, CA). An unstructured tetrahedral mesh is used, consisting of 1.9 million first-order volumetric elements. This mesh size was selected through a detailed grid-refinement study, comparing various unstructured tetrahedral mesh sizes ranges from 1.8 to 3.4 million tetrahedra. AcuSolve (ACUSIM software, Mountain View, CA) is employed to solve the algebraic form of the Reynolds-averaged Navier–Stokes equations at each of the nodes defined by the mesh. This solver uses a Galerkin least-squares finite element formulation with second order accuracy. The code implements the Spalart-Allmaras closure model for turbulence modeling and we require all of the weighted residuals of the governing equations to converge to less than 10^{-4}. Additional technical details regarding the use of this CFD code for investigations of stirred tanks can be found elsewhere (Johnson and Bittorf, 2002). Particle tracking is accomplished using commercially available software provided by ACUSIM. Subsequent mixing analysis is performed using custom software developed at the Pharmaceutical Engineering Program at Rutgers University (Zalc, 2000; Zalc et al., 2001).

2.2. Experimental flow characterization

Particle image velocimetry (PIV) is a quantitative, non-intrusive technique that is used to measure the planar velocity components for vertical planes within the stirred vessel. Mixing patterns are revealed using planar laser induced fluorescence (pLIF), a visualization technique in which structures along two-dimensional planes within the stirred vessel are exposed. Details regarding both techniques can be found in a recent article by Kukura et al. (Kukura et al., 2003).

2.3. Dissolution experiments

Dissolution studies are performed using three tablet types: rapidly disintegrating 10-mg prednisone calibrator tablets (USP Lot 00C056, Rockville, MD), non-

disintegrating 300-mg salicylic acid calibrator tablets (USP Lot O, Rockville, MD) and slow-disintegrating 220-mg naproxen sodium tablets (CVS Pharmacy Inc., Lot 2LE0445, Woonsocket, RI) purchased from a local pharmacy. The USP paddle method is followed using a standard 1 l dissolution vessel and 7.5-cm diameter paddle (SOTAX Corporation, Horsham, PA), assembled as per the USP 24 physical test section on dissolution (U.S. Pharmacopeial Convention, 2000). The studies are conducted at ambient temperature (19–20 °C) using the media specified in the USP monograph for each tablet. The tablet location is carefully controlled by preparing a circular ring on the inner dish of the dissolution vessel using silicone glue, 11 mm in diameter, in which the tablet could be placed. Two positions are tested; one in which the tablet is centered at the bottom of the vessel, the other in which the ring is positioned 21 mm from the center, selected to correspond to locations of minimum and maximum shear, respectively. The tablet is placed in the silicone ring prior to the addition of dissolution medium. The solution is then added slowly to the vessel, trying to minimize any dissolution. To account for any dissolution that may occur from the medium addition, a sample is removed from the vessel prior to initiating the experiment. During the experiment, samples are manually removed from the vessel at 5-min intervals for a total of 45 min. At each time point, one 3-ml aliquot is removed, taken from the middle region of the dissolution vessel (typically referred to as the sampling zone). Immediately upon sampling, the contents are filtered using a 0.22-μm filter and stored in a parafilmed vial until analyzed. The volume of medium removed at each time point is not replaced as specified by the USP guidelines since the goal of these tests was solely to compare the various tablet positions. Five experiments are performed for each tablet position to establish reproducibility and determine the statistical significance of any differences in dissolution rates. The samples are analyzed by UV spectrophotometry using a UV-1601 UV–vis Spectrophotometer (Shimadzu Corporation, Columbia, MD) at the specified wavelength (see Table 1) and compared against a reference standard solution with a known concentration.

2.4. Data analysis

Comparison of dissolution profiles in this study is accomplished via two methods; a model independent approach using similarity and difference factors, and an analysis of variance (or a standard Student's *t*-test) is performed at each time point. Model dependent approaches cannot be utilized since the volume of the dissolution medium is not replenished during sampling.

In 1996, Moore and Flanner (Moore and Flanner, 1996) proposed a model-independent mathematical approach to compare dissolution profiles using two factors, f_1 and f_2. This method has been adopted by the Center for Drug Evaluation and Research (CDER) and by Human Medicines Evaluation Unit of The European Agency for the Evaluation of Medicinal Products (EMEA) as a criterion for assessing similarity between dissolution profiles, with the primary focus on the f_2 comparison in Agency guidelines (Shah et al., 1999). The two factors, referred to as the difference and similarity factors, respectively, are given in Eqs. (3) and (4), where R_t and T_t are the cumulative percent of drug dissolved at each of the selected n time points of the reference and test products, respectively.

$$f_1 = \left\{ \frac{(\sum_{t=1}^{n} |R_t - T_t|)}{(\sum_{t=1}^{n} R_t)} \right\} \times 100 \tag{3}$$

$$f_2 = 50 log \times \left\{ \left[1 + \left(\frac{1}{n} \right) \sum_{t=1}^{n} (R_t - T_t)^2 \right]^{-0.5} \times 100 \right\} \tag{4}$$

Table 1
Experimental conditions for dissolution sampling studies

Tablet	Type	Dissolution medium	Medium volume (ml)	Agitation speed (rpm)	UV wavelength (nm)
Prednisone (calibrator)	Disintegrating	DI water	500	50	242
Salicylic acid (calibrator)	Non-disintegrating	Phosphate buffer (pH 7.4)	900	100	296
Naproxen sodium	Slow-disintegrating	Phosphate buffer (pH 7.4)	900	50	332

The FDA has set a public standard of f_2 values between 50 and 100 and f_1 values between 0 and 15 to indicate similarity of two curves. In keeping with established procedures, the f_1 and f_2 factors are calculated and presented for the data communicated in this paper. For this study, the factor analysis is performed using an averaged centered profile and an averaged off-centered profile.

Subsequently, a rigorous approach is used to assess the true statistical nature of the data. JMP statistical software is utilized for a rigorous analysis of the dissolution data. A one-way analysis of variance is used to compare the data from the two tablet positions at each time point. To verify that the assumption of equal variances is met for each time point, a Levene test is also performed. In the instances when the Levene test indicates that the two variances are not equal, Welch's ANOVA (or Welch's approximate *t*-test) is employed. Welch's approximate *t*-test is a common statistical technique used to compare the means of two populations with different variances. This statistic is calculated using Eq. (5). The hypothesis test is then based on comparing t' to the normal critical value of the Student's *t*-distribution with the calculation for the degrees of freedom shown in Eq. (6):

$$t' = \frac{\overline{x_1} - \overline{x_2}}{\sqrt{(s_1^2/n_1) + (s_2^2/n_2)}} \tag{5}$$

$$\upsilon' = \frac{((s_1^2/n_1) + (s_2^2/n_2))^2}{((s_1^2/n_1)^2/(n_1 - 1) + (s_2^2/n_2)^2/(n_2 - 1))} \tag{6}$$

3. Results

3.1. Development of a CFD model

Fig. 1a depicts the two-dimensional time-averaged velocity field for the fluid within the dissolution device at a Reynolds number of 4688, corresponding to mixing an aqueous solution at 50 rpm. Similarly, Fig. 1b shows the velocity field for a Reynolds number of 9375, corresponding to the agitation of an aqueous medium at 100 rpm. The vectors in the two figures are scaled, using different scaling factors, according to their magnitudes. The overall circulation patterns observed in the two figures are similar. On average, material is ejected

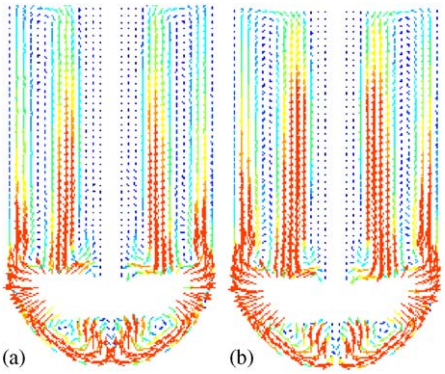

Fig. 1. Two-dimensional, time-averaged CFD velocity fields for (a) *Re* = 4688, and (b) *Re* = 9375.

from the paddle and is either directed up the wall to the top of the vessel before returning down a channel midway between the shaft and the wall, or fluid is pushed down to the bottom dish along the wall before moving up to the paddle in the center of the device. Recirculating regions, first reported by Bocanegra et al. (Bocanegra et al., 1990) as a secondary flow in the device, are evident both above and below the paddle.

While velocity fields provide valuable information describing the overall fluid flow patterns and long-term recirculation zones, they offer no information regarding short-time mixing dynamics. Particle tracking simulations are utilized to illustrate the evolution of mixing (Fig. 2a) at a Reynolds number of 4688 (50 rpm). The initial condition of the particle tracking is a sphere of points placed just above the paddle, chosen to mimic

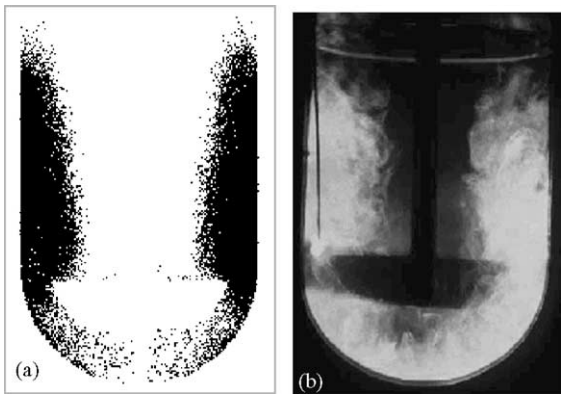

Fig. 2. (a) Particle tracking simulation results for *Re* = 4688 after 6 s of agitation, (b) pLIF visualization experiment at *Re* = 4688.

the location of dye injection in the corresponding pLIF experiment. Whenever a particle crosses the plane parallel with the agitator blade at the center of the vessel, the particle-tracking algorithm plots its position. All of the intersections made during the first 6 s of mixing are shown in Fig. 2a. Unlike the mixing patterns observed under laminar conditions, the mixing patterns in Fig. 2a show a disorganized mixture structure typical of turbulence where the transport of momentum and energy is accomplished through eddies of different length scales and consequently large-scale stretching and folding patterns are not formed (as in the case of the laminar regime) (Kukura et al., 2003). Analogous to the particle tracking simulations, dye advection experiments unveil flow patterns and coherent structures that serve as a starting point to analyze fluid mixing. The mixing process can be assessed by examining the location of tracers in both time and space. Fig. 2b shows an image from a pLIF experiment conducted in an aqueous solution agitated at 50 rpm. The picture was taken a few seconds after injecting the dye above the paddle blade. Consistent with the particle tracking simulation in Fig. 2a, the dye travels quickly up the wall above the paddle and only later fills the region surrounding the shaft. The dye is also transported to a small region below the center of the paddle more slowly than outer areas. The excellent agreement between the experiment and simulation evidenced in Fig. 2 demonstrates that the model accurately captures the flow physics, and that it can be used with confidence in subsequent analysis. Extensive validation of the ACUSIM solver in stirred tanks can readily be found in the literature, providing additional confidence in the use of the model (Zalc, 2000; Zalc et al., 2001; Johnson and Bittorf, 2002).

3.2. The velocity field in the USP apparatus II

Instantaneous velocity vector fields captured by PIV highlight the time-dependency of the flow in the USP apparatus II. Fig. 3a–c presents three velocity fields, captured 630 ms apart at a Reynolds number of 5013, corresponding to three consecutive half-rotations of the agitator. The vectors in each of the images are scaled with the same scale factor according to their magnitudes. Additionally, the vectors are color-coded in order of increasing velocity magnitude. The vectors with the lowest velocities are plotted in dark blue, followed by light blue, green, yellow, orange and red, which correspond to vectors with the highest velocities. As evident in Fig. 3a–c, substantial fluctuations in the flow are observed. An important feature of the transitional regime is the presence of eddies of different length scales. These eddies have large variations in velocity and are thought to contain the bulk of the kinetic energy in the system. Interactions of these large eddies with slower moving streams produce smaller eddies of higher frequency. Although the random, unsteady nature of the turbulent velocity field is desirable from a micromixing standpoint, the large-scale fluctuations in the flow can be detrimental to hydrodynamic uniformity within the system. These large flow fluctuations in the velocity field may be highly undesirable for testing consistency. The macro-scale unstable regions are of the same size as the tablets, which means that they have enough momentum to affect the motion of tablets and tablet fragments. This uncontrolled, heterogeneous release of solids creates a potential for inconsistent test results purely due to hydrodynamic conditions.

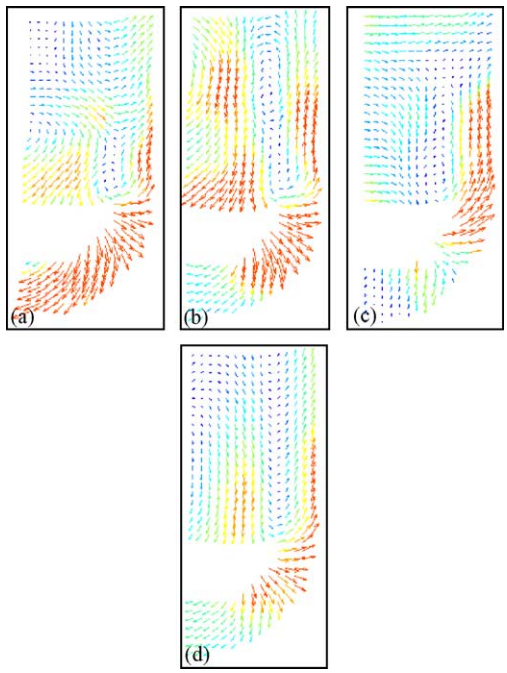

Fig. 3. Two-dimensional PIV velocity fields for $Re = 5013$ (a–c) instantaneous PIV velocity fields, taken 630 ms apart, (d) time-averaged PIV velocity field.

To better illustrate this point, a visualization experiment is performed with a salicylic acid tablet contain-

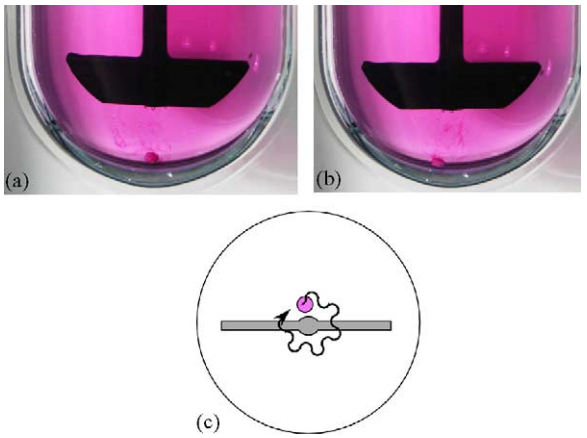

Fig. 4. Visualization of tablet movement in the USP dissolution test under typical operating conditions. (a and b) Photographs of tablets movement during visualization experiments, and (c) illustration of tablet movement during the experiment.

ing 3 wt.% phenolphthalein.[2] The tablet, 6.5 mm in diameter, is dropped into the dissolution vessel filled with 0.1N sodium hydroxide solution and allowed to settle. The agitator is started at 50 rpm and the movement of the tablet is observed from the bottom of the tank. During the experiment the tablet is observed to move in a circular fashion, following the direction of the paddle rotation. In addition to the rotation around the dish, the tablet is observed to move to the center of the dish and out again in what appears to be an erratic motion. Fig. 4a and b shows two photographs taken during the experiment, as viewed from the side of the vessel. In Fig. 4a, the tablet is photographed in the center of the dish. However, moments later the tablet is observed in an off-centered position as shown in Fig. 3b. Fig. 4c depicts an illustration of the observed trajectory of the tablet during the dissolution experiment, as monitored from the bottom dish of the vessel. The maximum distance from the center that this particular tablet was observed to travel was 11 mm, however, other tablets showed different motion patterns. While the degree and exact path of the tablet movement is likely a function of a number of variables such as tablet shape, size, thickness, density and initial placement, it is apparent that a tablet will not necessarily remain stationary throughout the test.

[2] Phenolphthalein is used as an indicator to make the tablet movement visibly more clear and easier to photograph.

In order to demonstrate the agreement between CFD results and experimental measurements of the flow patterns in the dissolution device, the time-averaged, two-dimensional velocity fields are compared for a vertical plane aligned with the paddle. Averaging 50 instantaneous PIV vector fields yields a time-averaged velocity field, presented in Fig. 3d, which can then be compared with the CFD results from Fig. 1a. While local details differ due to the different averaging procedures in PIV and CFD, both the computational and experimental results indicate that two recirculation loops exist, with one located above and one located below the agitator. Both plots also show that the fluid is ejected radially to the vessel wall and then either flows up towards the liquid surface before returning down or is pushed down to the lower dish until it flows up to the paddle in the center of the vessel. Additionally, it can be noted from both vector fields that in the region directly next to the agitator shaft, fluid flow is significantly slower that in the other regions of the vessel.

3.3. Distribution of shear forces

Experiments conducted by Hamlin et al. (Hamlin et al., 1962) have shown that variation in the boundary layer thickness due to changing agitation speeds can compromise the ability of the in vitro dissolution test to predict in vivo performance. The thickness of the boundary layer at the surface of the tablet is controlled by the shear forces exerted by the fluid. Fig. 5a and d shows the distribution of strain rates in the plane of the paddle at Reynolds numbers of 4688 and 9375, respectively. The contour plots show substantial spatial heterogeneity in the shear rate for both Reynolds numbers. In fact, changing the agitator speed in the usual operating range only affects the magnitude of the shear forces and appears to have negligible impact on the spatial distribution of strain rates. In both cases, the highest deformation rate exists at the surface of the paddle. Additionally, the vessel wall experiences high shear rate relative to the interior of the tank. The lowest shear is observed between the agitator shaft and the vessel wall above the paddle. Fig. 5b and c illustrates the instantaneous strain distribution along the wall of the vessel at $Re = 4688$, shown from the side and bottom views, respectively. Corresponding images for $Re = 9375$ are depicted in Fig. 5e and f. Once again, substantial spatial heterogeneity is observed. The most striking observa-

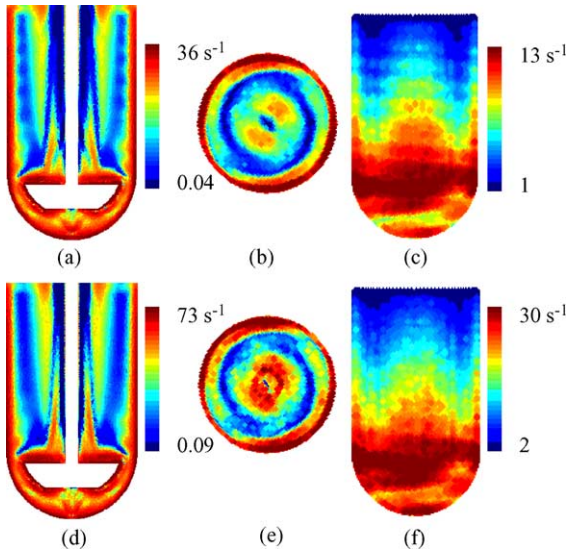

Fig. 5. Distribution of strain rates for $Re = 4688$ (a) in the fluid, (b) along the wall, depicted from a bottom view of the dish, (c) along the wall, depicted from a side view of the entire vessel; and for $Re = 9375$, (d) in the fluid, (e) along the wall, depicted from a bottom view of the dish, (f) along the wall, depicted from a side view of the entire vessel.

tion from Fig. 5b and e is the presence of a circular low-shear region at the bottom center of the device, corresponding to the most probable location of a tablet during the dissolution test. Outside of this small area, the shear forces rise rapidly. Fig. 6 shows the rate of strain (averaged in the azimuthal direction) versus distance along the wall from the bottom of the dish for both $Re = 4688$ and 9375. The figure depicts steep changes in the shear intensity within the dish bottom of the vessel. The highest shear rates are observed at the height of the paddle and the intensity gradually decays along the wall.

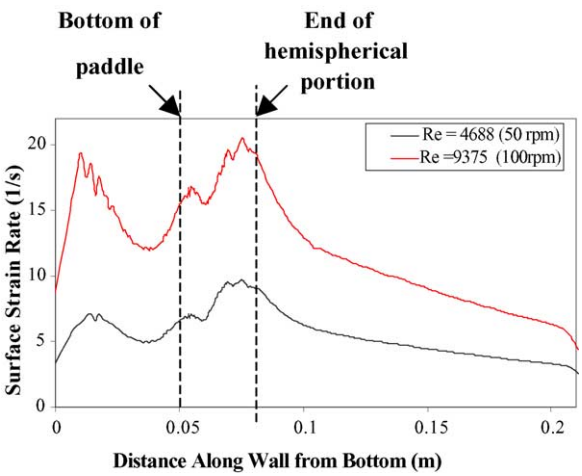

Fig. 6. Average rate of strain along the wall as a function of distance.

3.4. Dissolution experiments

To demonstrate the impact that non-uniform shear forces can have on dissolution testing, experiments that measure the dissolution rates at two distinct and fixed tablet locations were conducted. Using the shear distribution plot in Fig. 6, centered and off-centered (21 mm from center) locations were selected, corresponding to minimum and maximum shear, respectively. Fig. 7a shows a graph of the prednisone concentration versus time for the prednisone calibrator tablets at the two tablet locations. The first observation to note is the high variability observed at the zero time point. The cause of this variability stems from the experimental method used, specifically placing the tablet in the vessel before the addition of the dissolution media. Due to the rapid disintegrating nature of the prednisone tablets, some disintegration and subsequent dissolution occurs as a result of addition of the aqueous medium. However, statistical analysis shows that there is no significant difference between the dissolution at the zero time point for tablets in the centered position versus those in the off-centered position. Comparing the overall experiments, more than a two-fold difference in the measured dissolution rate is observed between the experiments at the two tablet locations. Statistical analysis shows a difference factor of 146.2 and a similarity factor of 31.5, clearly indicating that the two profiles are not statistically similar by this technique. A more rigorous statistical analysis, presented in Table 2, shows that the two positions are statistically different at all time points greater than 5 min. At most of the time points, a Levene test indicates that the variances of the two populations are not equal, consequently the assumptions for ANOVA are no longer valid. For these time points, Welch ANOVA or Welch's modified *t*-test is used.

Fig. 7b shows the dissolution–time curve for the salicylic acid calibrator tablets. Once again, the dissolution rate is observed to be higher for the tablets measured in the off-centered position. Interestingly, considerably higher variability is noted in the experiments performed

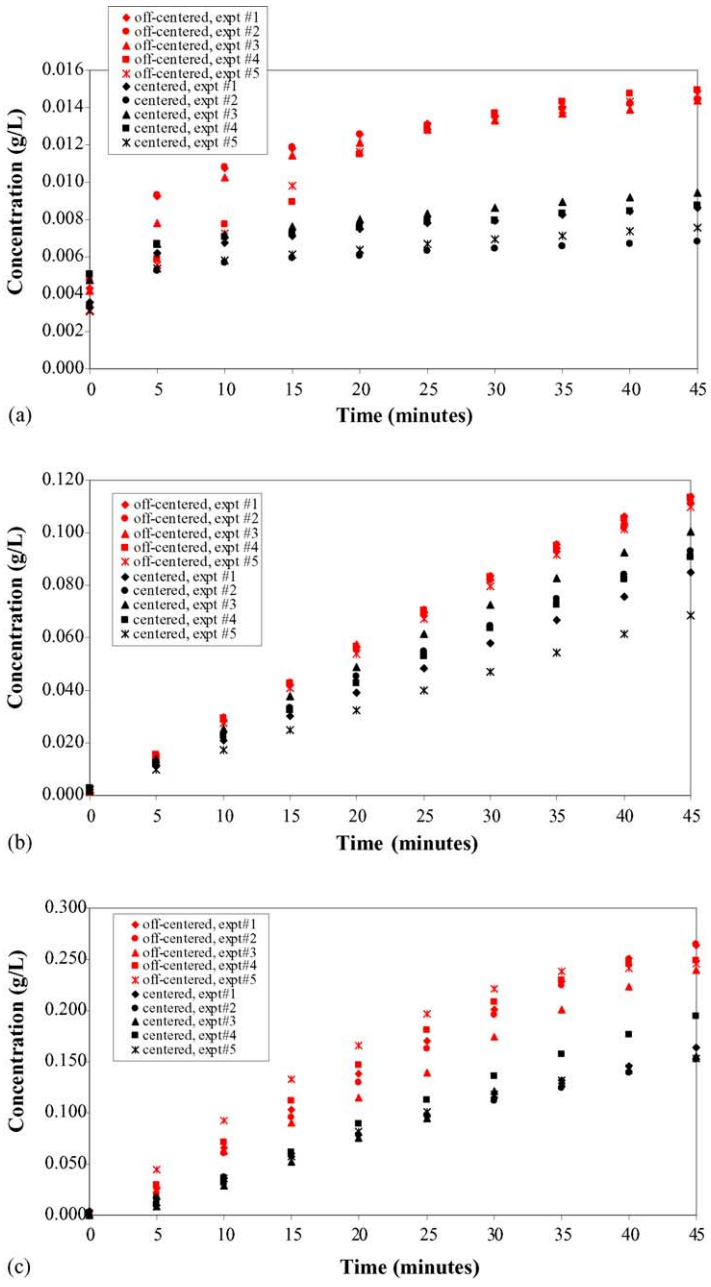

Fig. 7. Measured dissolution rate changes resulting from changes in tablet position for (a) prednisone calibrator tablets, (b) salicylic acid calibrator tablets, and (c) naproxen sodium tablets.

with the tablets in the centered position as compared to those conducted in the off-centered position. Comparison of the two curves via the fit factors yields conflicting results. The difference factor for salicylic acid is calculated to be 35.0, suggesting the curves are not similar. The similarity factor yields a value of 63.9, indicating that the two curves are in fact similar. Interpretation of these data by the FDA criteria

Table 2
Statistical analysis of dissolution sampling data

Sampling time (min)	Prednisone calibrator tablets				Salicylic acid calibrator tablets				Naproxen sodium tablets			
	F-ratio	$\Pr > F$	Levene test $\Pr > F$	Welch test $\Pr > F$	F-ratio	$\Pr > F$	Levene test $\Pr > F$	Welch test $\Pr > F$	F-ratio	$\Pr > F$	Levene test $\Pr > F$	Welch test $\Pr > F$
0	0.003	0.9582	0.302	NA	8.47	0.0196	0.921	NA	2.29	0.1688	0.781	NA
5	3.19	0.1117	0.027	0.132	21.49	0.0017	0.099	NA	17.51	0.0031	0.318	NA
10	11.72	0.0090	0.004	0.017	23.38	0.0013	0.108	NA	36.97	0.0003	0.145	NA
15	33.23	0.0004	0.063	NA	24.19	0.0012	0.065	NA	43.06	0.0002	0.043	0.0021
20	129.53	<0.0001	0.118	NA	24.62	0.0011	0.042	0.0063	44.12	0.0002	0.091	NA
25	205.98	<0.0001	0.002	0.0001	24.51	0.0011	0.052	NA	47.67	0.0001	0.125	NA
30	206.83	<0.0001	0.009	<0.0001	24.72	0.0011	0.051	NA	82.12	<0.0001	0.379	NA
35	189.08	<0.0001	0.008	<0.0001	25.37	0.0010	0.050	NA	108.64	<0.0001	0.966	NA
40	180.77	<0.0001	0.029	<0.0001	21.59	0.0017	0.052	NA	119.00	<0.0001	0.571	NA
45	177.46	<0.0001	0.015	<0.0001	20.33	0.0020	0.205	NA	88.27	<0.0001	0.577	NA

would likely lead the technician to conclude that tablet position does not significantly impact the dissolution rate of the salicylic acid calibrator tablets and the two sets would be considered similar. In contrast, the ANOVA method performed for salicylic acid, presented in Table 2, shows that the two positions are statistically different at all time points. The conflicting results obtained from the fit factor analysis further suggest that this analysis might not be sufficiently rigorous for all situations.

The dissolution–time curve for the naproxen sodium tablets is shown in Fig. 7c. A 70% average difference is observed between the experiments performed in the centered position and those performed in the off-centered position. A difference factor of 73.2 and a similarity factor of 28.1 both confirm the positions to be statistically different. ANOVA also shows the two positions to be statistically different at all time points along the curve.

4. Discussion

The USP apparatus II is designed and implemented such that during testing a tablet (or tablet fragment) may move about the device freely. Factors such as density, variations in initial placement, tablet size and shape would likely influence the motion of a tablet during testing. CFD modeling of the fluid flow within the dissolution device shows that substantial spatial heterogeneity in the rate of strain is present in the dissolution device under the standard operating conditions. In fact, at a Reynolds number of 4688 (agitated at 50 rpm) a two-fold difference in shear rate is observed between positions at the center of the dish and 21 mm off-center. This difference is even larger at higher agitation rates. Another result from these simulations is that the heterogeneity observed is not improved in any significant manner as the agitation speed is increased. The magnitudes of the velocities (and shear rates) are increased, however, the tremendous spatial fluctuations are not only still present but appear to be magnified.

The influence of the shear rate (or rate of deformation) on the boundary layer thickness is well known in the field of fluid mechanics. In general, the thickness of the boundary layer is inversely proportional to the fluid velocity and rate of strain. The dissolution of a solid dosage form is given by the application of Fick's

law, as shown in Eq. (7) below:

$$\frac{dM}{dt} = \frac{D}{h} A (C_S - C) \quad (7)$$

Here, M is the mass of drug to be dissolved, A the surface area exposed to the dissolution medium, D the dissolution coefficient, C_S the solubility of drug, C the drug concentration in the medium and h is the thickness of the diffusion boundary layer. Studies in the literature have shown that boundary layer thickness can directly influence dissolution rate measurements (Hamlin et al., 1962; Levy, 1963; Mauger, 1996). Consequently, variations in the rate of shear can greatly affect dissolution measurements in the USP device. The dissolution experiments in this study, conducted using three different types of tablets, strongly support this notion. The experiments are performed at two fixed tablet locations, positioned 0.02 m apart. The prednisone calibrator tablets exhibit the greatest sensitivity to tablet position, yielding a two-fold difference in dissolution rate. This is likely due to the compounded effect of an increase in surface area due to the rapid disintegrating nature of the tablet, and the increased rate of deformation in the off-centered position. The naproxen sodium tablets, slow disintegrating in nature, are also observed to have an increased surface area in the off-centered position. The salicylic acid calibrator tablets show the least sensitivity to tablet location, likely because they do not disintegrate at all and maintained a more constant surface area throughout the test. In all three cases, hydrodynamic effects are shown to strongly influence the dissolution behavior.

The method used to analyze the dissolution data is another important consideration. While the fit factors are easy to use from an application and interpretation standpoint, only one value is obtained to explain the likeness of two dissolution profiles (Yuksel et al., 2000). Alternatively, ANOVA-based methods have tighter limits and are more discriminative since they provide a possibility for the multifactorial comparison of dissolution data on a point-by-point basis. As in the case of the salicylic acid calibrator tablets, the ability to compare the profiles at each time point may be necessary to determine the true likeness of the curves. Additionally, comparison on a point-by-point basis can provide useful information about changes that might occur during the various stages of dissolution that might be otherwise missed using a fit factor analysis.

In conclusion, a validated CFD model was used to demonstrate that the shear strain environment in the USP apparatus II under typical operating conditions is highly heterogeneous. Experiments have confirmed that dissolution rates can vary significantly when exposed to different shear environments. Specifically, three distinct tablet types were shown to have statistically significant dissolution rates when the tablets were fixed in two differing locations, only 2 cm apart, selected using the CFD model to maximize shear rate differences. Enormous differences in dissolution rates were observed as a function of position. These results aid in the understanding of the underlying hydrodynamics within the dissolution device and help to explain some of the variability often observed when using the USP apparatus II.

The USP has recently discussed potential changes in dissolution testing, including operation in the laminar regime, which may provide a more uniform hydrodynamic environment (USP Dissolution Meeting, January 2003). Evaluation of the dissolution environment in the manner demonstrated in this study will contribute to the development of more rigorous dissolution tests, potentially preventing many problems.

Acknowledgements

The authors wish to acknowledge the financial support of this project to the Schering-Plough Research Institute, Johnson and Johnson, Wyeth and to Merck & Co. Inc., for the support of Jennifer Baxter and Joseph Kukura during their doctoral studies. The authors also wish to thank John Reali, Zubia Naji and Ashley Alexandro for their efforts in the laboratory.

References

Bardina, J.E., Huang, P.G., Coakley, T.J., 1997. Turbulence Modeling, Validation, Testing and Development. NASA Technical Memorandum.

Bocanegra, L.M., Morris, G.J., Jurewicz, J.T., Mauger, J.W., 1990. Fluid and particle laser doppler velocity measurements and mass transfer predictions for USP paddle method dissolution apparatus. Drug Dev. Ind. Pharm. 16, 1441.

Cox, D.C., Furman, W.B., 1982. Systematic error associated with apparatus 2 of the USP dissolution test I: effects of physical alignment of the dissolution apparatus. J. Pharm. Sci. 71, 451.

FDC Reports, 2001. Recalls Prompted By FDA on the Increase. The Gold Sheet 35, 1.

FDC Reports, 2002. Counterfeits Pose Special Recall Challenge. The Gold Sheet 36, 1.

FDC Reports, 2003. Spike in Potency-Related Problems Contributes to Overall Rise in 2002 Recalls. The Gold Sheet 37, 1.

Hamlin, W.E., Nelson, E., Ballard, B.E., Wagner, J.G., 1962. Loss of sensitivity in distinguishing real differences in dissolution rates due to increasing intensity of agitation. J. Pharm. Sci. 51, 432.

Healy, A.M., McCarthy, L.G., Gallagher, K.M., Corrigan, O.I., 2002. Sensitivity of dissolution rate to location in the paddle dissolution apparatus. J. Pharm. Pharmacol. 54, 441.

Johnson, K., Bittorf, K.J., 2002. Validating the Galerkin least-squares finite element methods in predicting mixing flows in stirred tank reactors, Proceedings of the 10th Annual Conference of the CFD Society of Canada, Windsor, Ont., p. 490.

Kamba, M., Seta, Y., Takeda, N., Hamaura, T., Kusai, A., Nakane, H., Nishimura, K., 2003. Measurement of agitation force in dissolution test and mechanical destructive force in disintegration test. Int. J. Pharm. 250, 99.

Kresta, S.M., Brodkey, R.S., 2004. Turbulence in mixing applications. In: Paul, E.L., Atiemo-Obeng, V.A., KrestaHoboken, S.M. (Eds.), Handbook of Industrial Mixing: Science and Practice.

Kukura, J., Szalai, E., Arratia, P., Muzzio, F., 2002. Understanding pharmaceutical flows. Pharm. Technol. 26, 48.

Kukura, J., Arratia, P.C., Szalai, E.S., Muzzio, F.J., 2003. Engineering tools for understanding hydrodynamics of dissolution tests. Drug Dev. Ind. Pharm. 29, 231.

Levy, G., 1963. Effect of certain tablet formulation factors on dissolution rate of the active ingredient. J. Pharm. Sci. 52, 1039.

Levy, G., Leonards, J.R., Procknal, J.A., 1965. Development of in vitro dissolution tests which correlate quantitatively with dissolution rate-limited drug absorption in man. J. Pharm. Sci. 54, 1719.

Mauger, J.W., 1996. Physicochemical and fluid mechanical factors related to dissolution testing. Diss. Tech. 3, 7.

Mauger, J.W., Brockson, R., De, S., Gray, V.A., Robinson, D., 2003. Intrinsic dissolution performance of USP apparatus 2 using modified salicylic acid calibrator tablets: proof of principle. Diss. Tech. 10, 6.

Moore, J.W., Flanner, H.H., 1996. Mathematical comparison of dissolution profiles. Pharm. Technol. 20, 64.

Moore, T.W., Hamilton, J.F., Kerner, C.M., 1995. Dissolution testing: limitations of the USP prednisone and salicylic acid calibrator tablets. Pharm. Forum 21, 1387.

Qureshi, S.A., Shabnam, J., 2001. Cause of high variability in drug dissolution testing and its impact on setting tolerances. Eur. J. Pharm. Sci. 12, 271.

Shah, V.P., Tsong, Y., Sathe, P., Williams, R.L., 1999. Dissolution profile comparison using similarity factor, f2. Diss. Tech. 6, 21.

U.S. Pharmacopeial Convention, 2000. USP XXIV Rockville, MD, p. 1941.

Underwood, F., Cadwallder, D., 1976. Effects of various hydrodynamic conditions on dissolution rate determinations. J. Pharm. Sci. 65, 697.

Yuksel, N., Kanik, A.E., Baykara, T., 2000. Comparison of in vitro dissolution profiles by ANOVA-based, model-dependent and -independent methods. Int. J. Pharm. 209, 57.

Zalc, J.M., 2000. Computational Fluid Dynamics (CFD) Tools for Investigating Flow and Mixing in Industrial Systems: The Koch-Glitsch SMX Static Mixer and a Three Rushton Turbine Stirred Tank. Department of Chemical and Biochemical Engineering, Rutgers University, New Brunswick, NJ.

Zalc, J.M., Alvarez, M.M., Muzzio, F.J., 2001. Extensive validation of computed laminar flow in a stirred tank with three Rushton turbines. AIChE J. 47, 2144.